necrosis in 4, pneumonia in 1, lung embolism in 1, and pneumonitis in 1. The median OS of all patients was 20.0 months. The 1-, 2-, 3-, 4-, and 5-year survival rates were 69.6%, 42.8%, 26.5%, 13.3%, and 6.6%, respectively (Fig. 3A). The presence of a methylated *MGMT* gene promoter was significantly correlated with longer patient survival (HR, 2.42; 95% CI, 1.10-6.08; $P=.026$) (Fig. 3B), but no other patient- or treatment-related variables were associated with survival (Table 2). Subgroup analyses of patient survival are summarized in Table 3.

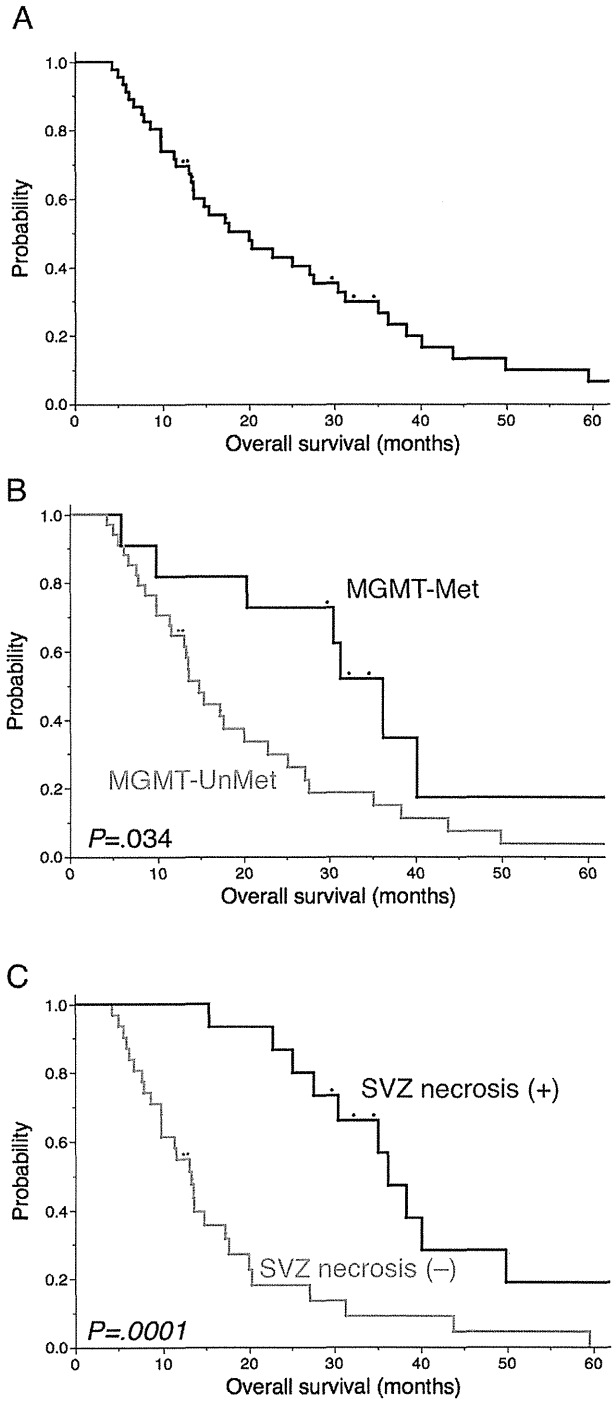

Fig. 3. Overall survival of the 46 patients. The median survival time was 20.0 months (A). Methylation (Met) of the *O-6-methylguanine-DNA methyltransferase* (MGMT) gene promoter (B) and necrosis in the subventricular zone (SVZ) (C) were significantly correlated with better survival (log–rank $P=.034$ and .0001, respectively).

Toxicity

No grade ≥3 adverse events were observed during IMRT. However, during and after treatment, radiation necrosis was frequently observed. This necrosis arose not only surrounding the original tumor site (Fig. 1D) but also in the SVZ, although this area was not included in the high-dose field (Fig. 1E). The incidence of radiation necrosis was 10.9% surrounding the original tumor, 21.7% in the SVZ, and 10.9% in both. The median time to necrosis was 42.0 months (95% CI, 28.1 months to not reached) at the original tumor site and 16.1 months (95% CI, 12.2 months to not reached) in the SVZ. The occurrence of radiation necrosis was not associated with the methylation status of the *MGMT* gene promoter: the HR was 1.40 at the original tumor site ($P=.641$) and 0.57 in the SVZ ($P=.278$).

Radiation necrosis in the SVZ was strongly associated with prolonged patient survival. The median OS was 36.2 and 13.3 months in patients with and without SVZ necrosis, respectively (HR, 4.08; 95% CI, 1.97-9.10; $P=.0001$) (Fig. 3C). Radiation necrosis at the original tumor site also showed a tendency to correlate with better survival, but this difference was not statistically significant (HR, 1.94; 95% CI, 0.91-4.61; $P=.089$). In multivariate analysis, SVZ necrosis was the only variable significantly associated with prolonged survival after hypofractionated high-dose IMRT (Table 2).

Hematologic toxicities secondary to chemotherapy or antiepileptic drugs were also observed during the treatment, as follows: grade 3 liver dysfunction in 8 patients (17.8%), grade 3 or 4 anemia in 8 (17.8%), grade 3 or 4 lymphocytopenia in 21 (45.7%), grade 3 or 4 neutropenia in 3 (6.5%), and grade 3 thrombocytopenia in 1 (2.2%).

Discussion

Nakagawa et al (5) reported alteration of the failure pattern of GBM from local to disseminated by dose escalation to 90 Gy by 3-dimensional conformal radiation therapy (3D-CRT), which indicated better local tumor control by high-dose radiation therapy. However, Chan et al (6) reported no local control benefit with 90 Gy by 3D-CRT. Several other investigators also failed to prove a survival benefit of dose escalation with 70 Gy (7), 78 Gy (8), and 84 Gy (9) by 3D-CRT. Therefore, the effect of dose escalation with conventional 1.8- to 2.0-Gy fractions is still being debated.

Hypofractionation is a different approach to increase the biological effect of irradiation (10). It has several advantages over conventional fractionation. First, increased cell damage by a higher dose per fraction is expected from a linear-quadratic (LQ) model. Second, the shortened treatment time may reduce the effect of rapid tumor repopulation during treatment (11). In GBM, the potential tumor-doubling time is reportedly ≤10 days (12, 13), and the effect of repopulation cannot be ignored. In addition to these advantages, the shortened treatment time may contribute to fewer hospitalized days.

However, hypofractionation has an increased risk of late toxicity of normal brain tissue. Therefore, recent trials have attempted to deliver doses focusing on a limited area using IMRT. Sultanem et al

Table 2 Survival analyses

Variables	High-risk group	Univariate analysis		Multivariate analysis	
		Hazard ratio (95% CI)	*P*	Hazard ratio (95% CI)	*P*
Age, y	<60	1.32 (0.64-2.60)	.441		
Sex	Male	1.51 (0.75-3.29)	.261		
KPS (%)	<70	1.42 (0.74-2.75)	.291		
Extent of resection	<95%	1.44 (0.71-2.82)	.303		
RPA class (III/IV vs (V/VI)	V/VI	1.52 (0.79-3.05)	.215		
MGMT	UnMet	2.42 (1.10-6.08)	.026	1.57 (0.68-4.11)	.305
Necrosis (regional)	No	1.94 (0.91-4.61)	.089	1.70 (0.76-4.33)	.205
Necrosis (paraventricular)	No	4.08 (1.97-9.10)	.007	4.71 (2.08-11.55)	.0002

Abbreviations: CI = confidence interval; KPS = Karnofsky performance status; MGMT = *O-6-methylguanine-DNA methyltransferase* gene; RPA = recursive partitioning analysis; UnMet = unmethlylated.

(14) reported on their hypofractionated IMRT with 60 Gy in 3.0-Gy fractions. IMRT with 50 Gy in 5.0-Gy fractions was also reported by Floyd et al (15). In the above 2 trials, hypofractionation contributed to a shortened treatment period, but the biologically effective doses (BEDs) calculated based on the LQ model (alpha/beta = 10; 78 Gy in the trial by Sultanem et al [14], 75 Gy in the trial by Floyd et al [15]) were equivalent to that of conventional irradiation (72 Gy), and failed to improve patient survival. In contrast to these reports, we previously reported the benefits of dose escalation using hypofractionated IMRT (16). In that report, the dose for the central lesion was escalated from 48 Gy (BED, 77 Gy) to 68 Gy (BED, 126 Gy), and we demonstrated a favorable effect on local control without severe early toxicities. From these results, we fixed the dose at 68 Gy and used the same fractionation scheme: 8 fractions during 10 treatment days.

More recently, trials of dose escalation using hypofractionated IMRT with concurrent and adjuvant TMZ have been reported. In a study by Chen et al (17), all patients received a total dose of 60 Gy, but the dose per fraction was escalated from 3.0 to 6.0 Gy in 1.0-Gy increments. Their median patient survival was 16.2 months, and acute toxicity secondary to irradiation was extremely rare. A recent report by Tsien et al (18) also demonstrated the safety of hypofractionated IMRT. In our current series, we experienced no acute toxicity related to irradiation. In contrast to previous reports, our hypofractionated high-dose IMRT altered the dominant failure pattern from local to disseminated. A decreased incidence of local failure after high-dose irradiation has also been reported by several investigators. In addition to the report by Nakagawa et al (5) noted earlier, Tsien et al (18) reported a decreased probability of central failure with increased radiation doses. Intensive IMRT targeting regional tumors prolonged the time to local failure, but not to dissemination, resulting in earlier appearance of dissemination rather than local progression and alteration of the dominant failure pattern. Although our treatment still had limitations, the median patient survival was 20.0 months, and the 2- and 3-year survival rates were 42.8% and 26.5%, respectively. These survival results indicate the potential benefit of hypofractionated high-dose IMRT.

Late toxicities after our treatment were more frequent than early toxicities, and careful observation was required. Radiation necrosis was the most frequent late toxicity, and symptomatic necrosis requiring necrotomy developed in 5 patients. Surprisingly, these necroses progressed more frequently and much earlier in the SVZ than at the original tumor site, although SVZ was not included in the high-dose field. The irradiated doses to the SVZ were equivalent to 50 to 60 Gy of conventional radiation (alpha/beta = 3). Hypofractionated radiation might have a higher risk of SVZ injury than expected by the LQ model.

Table 3 Subgroup analyses of patient survival

	Median, mo (95% CI)	2 y (%)	3 y (%)	4 y (%)	5 years (%)
Overall (46)	20.0 (13.3-27.6)	42.8	26.5	13.3	6.6
Extent of surgery					
Complete resection (29)	20.0 (13.6-30.4)	46.1	26.3	13.2	8.8
Partial resection (17)	11.4 (5.9-38.3)	39.2	29.4	14.7	0.0
Age, y					
<50 (3)	20.4 (11.4-49.9)	33.3	33.3	33.3	0.0
50-60 (11)	20.0 (11.6-25.1)	31.8	0.0	0.0	0.0
>60 (32)	17.2 (9.8-36.2)	47.5	35.9	15.4	10.3
RPA					
Class IV (17)	25.1 (11.4-59.6)	51.3	36.7	24.5	12.2
Class V (16)	21.4 (7.9-36.2)	43.8	29.2	7.3	7.3
MGMT methylation					
Unmethylated (34)	14.8 (11.4-22.8)	29.9	15.0	7.5	3.7
Methlyated (11)	36.2 (9.8-not reached)	72.7	52.0	17.3	17.3

Abbreviations: CI = confidence interval; MGMT = *O-6-methylguanine-DNA methyltransferase* gene; RPA = recursive partitioning analysis.

On the other hand, the SVZ is believed to harbor cancer stem cells (CSCs) in patients with GBM (19, 20). Increased dose delivery to the SVZ (≥59.4 Gy) has recently been reported to correlate with better tumor control (21-23). However, CSCs may reportedly be resistant to radiation therapy because of preferential activation of the DNA damage checkpoint and DNA repair response (24). It is difficult to believe that conventional radiation may directly control CSCs in the SVZ, but impairment of CSC niches may sterilize the function of CSCs and decrease the supply of mature glioblastoma cells. In our current series, SVZ injury was strongly associated with patient survival. Hypofractionated radiation had a higher risk of SVZ injury, but it also had a stronger effect on impairment of CSC niches, which resulted in better patient outcomes. However, the SVZ also harbors neural stem cells, and injury to this area may increase the risk of neurocognitive sequelae. Several studies have recently reported a positive correlation between the radiation dose to the hippocampus and cognitive function in series of pediatric brain tumors (25-27). In our series, hippocampus injury was observed in only 1 patient, and the majority of necroses were observed in the SVZ of the anterior horn (6 patients), body (7 patients), and occipital horn of the lateral ventricle (1 patient). However, SVZ necrosis progressed after irradiation, and the performance status of the patients was impaired as necrosis progressed. Although it progressed very slowly, SVZ injury was the major cause of deterioration in the performance status of long-term survivors. Whether we should escalate the irradiation dose to the SVZ to control CSCs or spare this area to protect neural stem cells remains controversial.

Recent reports have indicated the usefulness of Met-PET to distinguish tumor recurrence from necrosis with excellent sensitivity (75%-100%) and specificity (60%-100%), although different T/N cutoff ratios (1.58-1.90) have been used (28-31). In this study, Met-PET was available in 22 cases; 16 lesions were diagnosed as necrosis, and the remaining 6 were diagnosed as tumor recurrence with a T/N threshold of 1.8. Among these lesions, the pathologic diagnosis was confirmed in 9 cases: 3 SVZ necroses, 1 regional necrosis, 2 local recurrences, and 3 disseminated diseases. No discrepancies in diagnosis were observed between Met-PET and pathologic analysis. However, another patient experienced regrowth of the lesion even though it had been diagnosed as necrosis by Met-PET 8 months before progression. We should be aware of the limitation of tracer imaging in that it reflects only the dominant features of lesions.

This single-institution prospective study demonstrated a satisfactory effect of hypofractionated high-dose IMRT on local control and survival in patients with GBM in the TMZ era. Despite the significant effect on control of GBM, this method still has some limitations. First, our IMRT contributed to local tumor control but not to prevention of dissemination. Second, our treatment increased the risk of radiation injury to the SVZ. The SVZ injury was associated with better patient survival but with impairment of patients' performance status. Third, this was a single-institution, small, nonrandomized study. Larger multiinstitutional randomized trials are required to validate our results and to confirm the efficacy of hypofractionated high-dose IMRT on control of GBM.

References

1. Stupp R, Hegi ME, Mason WP, et al. Effects of radiotherapy with concomitant and adjuvant temozolomide versus radiotherapy alone on survival in glioblastoma in a randomised phase III study: 5-year analysis of the EORTC-NCIC trial. *Lancet Oncol* 2009;10:459-466.
2. Sherriff J, Tamangani J, Senthil L, et al. Patterns of relapse in glioblastoma multiforme following concomitant chemoradiotherapy with temozolomide. *Br J Radiol* 2013;86:20120414.
3. Hegi ME, Diserens AC, Gorlia T, et al. MGMT gene silencing and benefit from temozolomide in glioblastoma. *N Engl J Med* 2005;352:997-1003.
4. Lim DA, Cha S, Mayo MC, et al. Relationship of glioblastoma multiforme to neural stem cell regions predicts invasive and multifocal tumor phenotype. *Neuro Oncol* 2007;9:424-429.
5. Nakagawa K, Aoki Y, Fujimaki T, et al. High-dose conformal radiotherapy influenced the pattern of failure but did not improve survival in glioblastoma multiforme. *Int J Radiat Oncol Biol Phys* 1998;40:1141-1149.
6. Chan JL, Lee SW, Fraass BA, et al. Survival and failure patterns of high-grade gliomas after three-dimensional conformal radiotherapy. *J Clin Oncol* 2002;20:1635-1642.
7. Graf R, Hildebrandt B, Tilly W, et al. Dose-escalated conformal radiotherapy of glioblastomas: results of a retrospective comparison applying radiation doses of 60 and 70 Gy. *Onkologie* 2005;28:325-330.
8. Watkins JM, Marshall DT, Patel S, et al. High-dose radiotherapy to 78 Gy with or without temozolomide for high grade gliomas. *J Neurooncol* 2009;93:343-348.
9. Tsien C, Moughan J, Michalski JM, et al. Phase I three-dimensional conformal radiation dose escalation study in newly diagnosed glioblastoma: Radiation Therapy Oncology Group Trial 98-03. *Int J Radiat Oncol Biol Phys* 2009;73:699-708.
10. Hingorani M, Colley WP, Dixit S, et al. Hypofractionated radiotherapy for glioblastoma: Strategy for poor-risk patients or hope for the future? *Br J Radiol* 2012;85:e770-e781.
11. Wang JZ, Li XA. Impact of tumor repopulation on radiotherapy planning. *Int J Radiat Oncol Biol Phys* 2005;61:220-227.
12. Hlatky L, Olesiak M, Hahnfeldt P. Measurement of potential doubling time for human tumor xenografts using the cytokinesis-block method. *Cancer Res* 1996;56:1660-1663.
13. Furneaux CE, Marshall ES, Yeoh K, et al. Cell cycle times of short-term cultures of brain cancers as predictors of survival. *Br J Cancer* 2008;99:1678-1683.
14. Sultanem K, Patrocinio H, Lambert C, et al. The use of hypofractionated intensity-modulated irradiation in the treatment of glioblastoma multiforme: Preliminary results of a prospective trial. *Int J Radiat Oncol Biol Phys* 2004;58:247-252.
15. Floyd NS, Woo SY, Teh BS, et al. Hypofractionated intensity-modulated radiotherapy for primary glioblastoma multiforme. *Int J Radiat Oncol Biol Phys* 2004;58:721-726.
16. Iuchi T, Hatano K, Narita Y, et al. Hypofractionated high-dose irradiation for the treatment of malignant astrocytomas using simultaneous integrated boost technique by IMRT. *Int J Radiat Oncol Biol Phys* 2006;64:1317-1324.
17. Chen C, Damek D, Gaspar LE, et al. Phase I trial of hypofractionated intensity-modulated radiotherapy with temozolomide chemotherapy for patients with newly diagnosed glioblastoma multiforme. *Int J Radiat Oncol Biol Phys* 2011;81:1066-1074.
18. Tsien CI, Brown D, Normolle D, et al. Concurrent temozolomide and dose-escalated intensity-modulated radiation therapy in newly diagnosed glioblastoma. *Clin Cancer Res* 2012;18:273-279.
19. Barani IJ, Benedict SH, Lin PS. Neural stem cells: Implications for the conventional radiotherapy of central nervous system malignancies. *Int J Radiat Oncol Biol Phys* 2007;68:324-333.
20. Li SC, Vu LT, Ho HW, et al. Cancer stem cells from a rare form of glioblastoma multiforme involving the neurogenic ventricular wall. *Cancer Cell Int* 2012;12:41.
21. Evers P, Lee PP, DeMarco J, et al. Irradiation of the potential cancer stem cell niches in the adult brain improves progression-free survival of patients with malignant glioma. *BMC Cancer* 2010;10:384.
22. Lee P, Eppinga W, Lagerwaard F, et al. Evaluation of high ipsilateral subventricular zone radiation therapy dose in glioblastoma: A pooled analysis. *Int J Radiat Oncol Biol Phys* 2013;86:609-615.

23. Chen L, Guerrero-Cazares H, Ye X, et al. Increased subventricular zone radiation dose correlates with survival in glioblastoma patients after gross total resection. *Int J Radiat Oncol Biol Phys* 2013;86:616-622.
24. Bao S, Wu Q, McLendon RE, et al. Glioma stem cells promote radioresistance by preferential activation of the DNA damage response. *Nature* 2006;444:756-760.
25. Armstrong GT, Jain N, Liu W, et al. Region-specific radiotherapy and neuropsychological outcomes in adult survivors of childhood CNS malignancies. *Neuro Oncol* 2010;12:1173-1186.
26. Jalali R, Mallick I, Dutta D, et al. Factors influencing neurocognitive outcomes in young patients with benign and low-grade brain tumors treated with stereotactic conformal radiotherapy. *Int J Radiat Oncol Biol Phys* 2010;77:974-979.
27. Redmond KJ, Mahone EM, Terezakis S, et al. Association between radiation dose to neuronal progenitor cell niches and temporal lobes and performance on neuropsychological testing in children: A prospective study. *Neuro Oncol* 2013;15:360-369.
28. Tripathi M, Sharma R, Varshney R, et al. Comparison of F-18 FDG and C-11 methionine PET/CT for the evaluation of recurrent primary brain tumors. *Clin Nucl Med* 2012;37:158-163.
29. Glaudemans AW, Enting RH, Heesters MA, et al. Value of 11C-methionine PET in imaging brain tumours and metastases. *Eur J Nucl Med Mol Imaging* 2013;40:615-635.
30. Terakawa Y, Tsuyuguchi N, Iwai Y, et al. Diagnostic accuracy of 11C-methionine PET for differentiation of recurrent brain tumors from radiation necrosis after radiotherapy. *J Nucl Med* 2008;49:694-699.
31. Okamoto S, Shiga T, Hattori N, et al. Semiquantitative analysis of C-11 methionine PET may distinguish brain tumor recurrence from radiation necrosis even in small lesions. *Ann Nucl Med* 2011;25:213-220.

OPEN ACCESS Freely available online

PLOS ONE

Prognostic Factors for Survival in Patients with High-Grade Meningioma and Recurrence-Risk Stratification for Application of Radiotherapy

Shigeru Yamaguchi[1], Shunsuke Terasaka[1]*, Hiroyuki Kobayashi[1], Katsuyuki Asaoka[5], Hiroaki Motegi[1], Hiroshi Nishihara[2], Hiromi Kanno[2], Rikiya Onimaru[3], Yoichi M. Ito[4], Hiroki Shirato[3], Kiyohiro Houkin[1]

1 Department of Neurosurgery, Hokkaido University Graduate School of Medicine, Sapporo, Japan, **2** Department of Pathology, Hokkaido University Graduate School of Medicine, Sapporo, Japan, **3** Department of Radiation Oncology, Hokkaido University Graduate School of Medicine, Sapporo, Japan, **4** Department of Biostatistics, Hokkaido University Graduate School of Medicine, Sapporo, Japan, **5** Department of Neurosurgery, Teine-keijinkai Hospital, Sapporo, Japan

Abstract

Background: Radiotherapy for high-grade meningioma (HGM) is one of the essential treatment options for disease control. However, appropriate irradiation timing remains under debate. The object of this study is to discern which prognostic factors impact recurrence in HGM patients and to propose a risk-stratification system for the application of postoperative radiotherapy.

Methods: We retrospectively reviewed 55 adult patients who were diagnosed with Grade II and III intracranial meningioma. Cox regression models were applied to the analysis for impact on early recurrence in HGM patients without postoperative radiotherapy.

Results: Grade III malignancy ($P = 0.0073$) and transformed histology ($P = 0.047$) proved to be significantly poor prognostic factors of early recurrence by multivariate analysis. The other candidates for recurrence factors were Simpson Grade 3–5 resection, preoperative Karnofsky Performance status $<= 70\%$, and MIB-1 labeling index $>= 15\%$. According to these prognostic factors, postoperative HGM patients could be stratified into three recurrence-risk groups. The prognoses were significantly different between each group, as the 3-year actual recurrence-free rates were 90% in low-risk group, 31% in intermediate-risk group, and 15% in high-risk group.

Conclusion: We propose recurrence-risk stratification for postoperative HGM patients using clinically available factors. Our results suggest that the prognosis for patients with high-risk HGMs is dismal, whereas HGM patients belonging to the low-risk group could have favorable prognoses. This stratification provides us with the criteria necessary to determine whether to apply adjuvant radiotherapy to postoperative HGM patients, and to also help identify potentially curable HGMs without adjuvant radiotherapy.

Citation: Yamaguchi S, Terasaka S, Kobayashi H, Asaoka K, Motegi H, et al. (2014) Prognostic Factors for Survival in Patients with High-Grade Meningioma and Recurrence-Risk Stratification for Application of Radiotherapy. PLoS ONE 9(5): e97108. doi:10.1371/journal.pone.0097108

Editor: James Bradley Elder, The Ohio State University Medical Center, United States of America

Received February 17, 2014; **Accepted** April 15, 2014; **Published** May 12, 2014

Funding: The authors have no support or funding to report.

Competing Interests: The authors have declared that no competing interests exist.

* E-mail: terasas@med.hokudai.ac.jp

Introduction

Although meningiomas have become the most common primary brain tumor and the majority of these are considered histologically benign [1], there is low incidence of high-grade meningiomas (HGMs), defined as Grade II and Grade III by WHO classification, and their biological behaviors are occasionally unpredictable [2,3]. In particular, the aggressive nature of HGMs in the event of tumor relapse has been noted, and recurrent HGMs are generally difficult to manage.

Retrospective studies have demonstrated that adjuvant radiotherapy can contribute to a favorable prognosis for patients with HGM [2,4]. However, the optimal timing of radiotherapy remains unclear for many clinicians. Some studies recommend that patients for whom gross total resection of the HGM cannot be achieved should receive postoperative radiotherapy [5,6], whereas other reports recommend that all patients with HGMs should receive postoperative irradiation regardless of the extent of the resection [2,4]. Thus, the indication of postoperative radiotherapy for HGMs is only discussed with respect to the extent of resection. However, is the extent of resection a sufficient clinical prognostic factor, especially by itself, when we make a decision regarding irradiation timing for postoperative HGM patients?

To elucidate the influence of radiotherapy on treatment outcomes and to discuss suitable irradiation timing in patients with HGMs, we rigorously reviewed the clinical factors and outcomes of HGM patients treated at our institutions and paid special consideration to radiation timing. We performed multivariate analysis of clinical and pathological factors, which are typically available in the postoperative period, leading to the

identification of possible prognostic factors for the risk of recurrence for HGM patients without postoperative radiotherapy. Based on the results of this analysis, we propose a stratification of recurrence-risk. In addition, an important aim of this study was to identify the patient group that did not require postoperative radiotherapy using appropriate criteria.

Materials and Methods

Patients

This study was approved by the Internal Review Board on Ethical Issues of Hokkaido University Hospital and appropriate written informed consents were obtained from eligible patients. A retrospective review was performed at the Hokkaido University Hospital and our affiliated institutions on patients since 1995 that were over 20 years old with a histological diagnosis of HGM, including WHO Grade II (n = 42) and Grade III (n = 13). We referred to pathological reports to identify HGM patients, and their diagnoses were re-confirmed by senior neuropathologists (H.N. and H.K.) according to WHO 2007 criteria, as described below. Pediatric patients, spinal meningiomas, and radiation-induced meningiomas were excluded in this study.

Ultimately, there were 27 males and 28 females with a mean age of 60±15 years (range: 23–84). Regarding histological classification, Grade II meningiomas included two clear cell meningiomas and one chordoid meningioma, and Grade III meningiomas included one papillary meningioma and one rhabdoid meningioma on which we have reported previously [7]. In this study, we included patients with HGMs that were transformed from benign (Grade I) meningiomas at first presentation. Those tumors are defined as "transformed", whereas the tumors that were diagnosed as HGM at first presentation were defined as "de novo" [8]. Ten Grade II tumors were categorized as transformed HGM; the mean interval between benign and Grade II histology was 10±9 years (range: 1–30 years). There are no cases that had progressed directly from benign to Grade III included in this series. All patients' characteristics are shown in Table 1.

Clinical Parameters and Outcome Assessment

Tumor size was defined by the largest diameter of contrast enhancement on the preoperative imaging. Each patient's preoperative condition was assessed by the Karnofsky performance status (KPS). Tumor locations were categorized into five groups: convexity, found in 17 cases; parasagittal/falcine/tentorial, in 20 cases; sphenoid ridge, in 9 cases; skull base, in 5 cases; and other, in 4 cases including intraventricular (n = 2), orbital (n = 1), and interosseous (n = 1). The endpoints were recurrence-free survival (RFS) and overall survival (OS), which were measured from the time of first HGM diagnosis. In the patients with transformed HGM, their time interval from benign to high-grade was not included in the survival analysis. All patients were followed in our institutions until death or their last visit. The time of recurrence was defined as the development of either clinically and radiographically evident relapse, or tumor re-growth. Patients without event were regarded as censored observations at the last follow-up visit.

Treatment

Simpson Grades 1 and 2 resections were designated as gross total resection confirmed by both operation record and postoperative radiographic appearance [9]. Postoperative adjuvant radiotherapy was administered to 19 patients, while the remaining 36 patients had irradiation deferred in case of relapse or tumor re-growth. The patients with postoperative radiotherapy were classified into the "early" irradiation group, and the others were classified into the "deferred" irradiation group. Postoperative radiotherapy was administered at the discretion of the physician. At the time of this analysis, 15 out of 36 patients in the deferred irradiation group had received irradiation for recurrent tumors. In terms of radiotherapy, patients were treated with X-ray based radiotherapy. The range of cumulative irradiation dose were from 50 Gy to 60 Gy using 2.0 Gy as the daily dose. Patients with HGM who were treated by other radiotherapies, such as gamma-knife or Boron Neutron Capture therapy (BNCT), are not included in this series.

Pathological Examination

All patients were re-evaluated to confirm the pathological diagnosis according to WHO 2007 criteria by senior neuropathologists. They counted mitoses per 10 high-power fields (HPFs, ×400) and the 5 prognostic histological parameters of hypercellularity, macronucleoli, small cell formation, patternless architecture and necrosis as 0 (no) or 1 (yes). The sum of each parameter was designated as an atypical score. Cases with 4 or more mitoses per 10 HPFs or with an atypical score greater or equal to 3 correspond to atypical meningioma. Cases with an obviously malignant cytology resembling that of carcinoma, melanoma, high-grade sarcoma, or a markedly elevated mitotic index (20 or more mitoses per 10 HPFs) correspond to anaplastic meningioma [10]. Cellular proliferation was assessed using the MIB-1 labeling index by immunohistochemistry. The quantification of the MIB-1 labeling index was performed by H.K., who was blinded to the clinical information. Eventually, MIB-1 labeling was made available to index of 50 out of 55 cases.

Statistical Analysis

All statistical analyses were carried out in R statistical environment version 3.0.2. Continuous variable data were expressed with standard deviation (SD). The mean of continuous variables was compared by Welch two sample t-tests, the median of continuous variables was compared by Mann-Whitney U test or Kruskal-Wallis test, and the distribution of categorical variables was compared by Pearson's Chi-squared test or Fisher's exact test according to the counts of expected frequencies. Estimated survival curves were shown by Kaplan-Meier method, and a log-rank test was used for the comparison.

To analyze prognostic factors for the risk of recurrence in the deferred irradiation group, the patient and the treatment characteristics were evaluated for association with the time to recurrence using Cox proportional hazards regression model. The analyzed characteristics included the patient's age, gender, preoperative KPS, previous diagnosis of meningioma, location of the tumor, extent of resection, MIB-1 labeling index, and the histological grade. A hazard ratio, with 95% confidence intervals (CIs) from a Cox model, summarized the effect; a non-parametric CI was calculated by the Greenwood formula. In multivariate analysis, the factors for which the *P*-value was below 0.1 in univariate analysis were selected. The factor of the MIB-1 labeling index could not be applied in multivariate analysis due to significant correlation with the histological grade (P = 0.015, Fig. 1). Statistical significance was given to p-values <0.05.

Results

Patient characteristics

Table 1 shows the patient characteristics between the early irradiation group and the deferred irradiation group. In comparison to the deferred irradiation group, the number of Grade III

Table 1. Descriptive statistics of study samples by postoperative radiotherapy.

	All patients (n = 55)	Early RT group (n = 19)	Deferred RT group (n = 36)	P-value[a]
Age (year), mean ± SD	60±15	58±15	62±16	0.38[b]
Gender				0.13[c]
Male	27	12	15	
Female	28	7	21	
Preoperative KPS (%)				0.59[c]
80–100%	35	13	22	
<80%	20	6	14	
Location				0.46[d]
Convexity	17	4	13	
Parasagittal/Falcial/Tentorial	20	8	12	
Sphenoid ridge	9	2	7	
Skull Base	5	3	2	
Others	4	2	2	
Tumor size (cm), mean ± SD	5.4±1.8	5.4±1.9	5.3±1.8	0.91[b]
Benign meningioma at first presentation				0.74[c]
No (de novo)	45	16	29	
Yes (transformed)	10	3	7	
Extent of Resection (Simpson Grade)				0.23[d]
Grade 1	14	4	10	
Grade 2	12	2	10	
Grade 3–5	29	13	16	
Histology				0.10[d]
Grade II	42	12	30	
Grade III	13	7	6	
MIB-1 labeling index (%), mean ± SD	11.2±7.4	12.6±7.2	10.4±7.5	0.30[b]
Median follow-up period (months)	43.9	50.1	40.3	0.62[e]
Endpoint				
Recurrence (%)	34 (62%)	11 (58%)	23 (94%)	
Death (%)	17 (31%)	9 (47%)	8 (22%)	

Abbreviations: SD, standard deviation; RT, radiotherapy.
[a]Comparison between early irradiation group and deferred irradiation group.
P-values were calculated by [b]Welch t-test, [c]Pearson's Chi-squared test, [d]Fisher's exact test and [e]Mann-Whiteny.
U-test.
doi:10.1371/journal.pone.0097108.t001

meningioma patients is higher in the early irradiation group, but the difference is not statistically significant (P = 0.10). There were no significant differences with respect to other clinical factors, nor to the extent of the resection. 34 out of the 55 tumors were found to have recurred and 17 patients died as a result of tumor progression. The median follow-up period of all patients was 43.9 months (range: 3.1–182.9 months), and there was no significant difference in median follow-up period between the two groups (P = 0.62). 21 out of 36 patients in the deferred irradiation group did not require irradiation at the time of this analysis. The median follow-up period of these 21 patients was 36.4 months.

Prognostic factors in deferred irradiation group

To identify which clinical factors influenced the recurrence of HGMs, we analyzed the deferred irradiation group using the Cox model (n = 36, Table 2). According to multivariate analysis, two parameters were found to be significant poor prognostic factors of early recurrence: Grade III malignancy (P = 0.0073) and transformed histology (P = 0.047). Although Simpson Grade 3–5 resection was one of the candidates of poor prognostic factors in univariate analysis (P = 0.0034), the extent of resection was not found to influence tumor recurrence in multivariate analysis (P = 0.82). The other possible poor prognostic factor was poor preoperative KPS (P = 0.019, in univariate analysis). Although we could not apply the MIB-1 labeling index of the tumor in multivariate analysis, univariate analysis indicated that a high MIB-1 labeling index, defined as more than 15%, might be a possible candidate for a prognostic factor for early recurrence (P = 0.020).

Recurrence-risk stratification

Based on the analyzed results of the Cox model, we propose to stratify the recurrence-risk group according to these prognostic factors (Table 3). For the high-risk group, two classifiers are selected that were identified as significant poor prognostic factors by multivariate analysis: Grade III malignancy, and transformed histology. For the intermediate-risk group, three prognostic factors are selected as classifiers based on univariate analysis as follows:

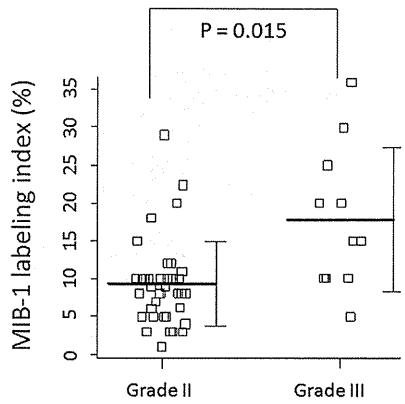

Figure 1. The MIB-1 labeling index of Grade II and Grade III meningioma. The mean MIB-1 labeling index of Grade II and Grade III meningioma are 9.3% and 17.8%, respectively, and these mean value are significantly different ($p = 0.015$). The bars represent the mean values and standard deviations.
doi:10.1371/journal.pone.0097108.g001

the patients with poor preoperative KPS, tumors with Simpson grade 3–5 resection, and high proliferative tumors suggested by high MIB-1 labeling index (more than 15%). The tumors that meet any of the above criteria are stratified into each recurrence-risk group, and the patients whose clinical and pathological characteristics do not match the above criteria are stratified into a low-risk group.

Figure 2 shows Kaplan-Meier curves of the patients in the deferred irradiation group according to the recurrence-risk stratification we propose. The prognosis shows a significant difference not only in RFS but also in OS among the recurrence-risk stratified groups ($p<0.001$ in PFS, $P = 0.001$ in OS). The 3-year actual recurrence-free rates of the low-risk, intermediate-risk, and high-risk groups were 90%, 31%, and 15%, respectively. In the intermediate-risk group, the median RFS is 28.4 months. Although the RFS of the intermediate-risk group was poor compared to the low-risk group, all patients who were stratified in intermediate-risk and low-risk group have been alive through follow-up periods. Finally, the prognosis of the high-risk group was dismal. The median RFS and OS of the high-risk group are 11.2 months and 52.1 months, respectively.

In addition, when the patients who received early irradiation had been assigned to this recurrence-risk stratification, 10 out of 19 tumors fell into the high-risk group, and 9 out of 19 tumors were in the intermediate-risk group. Figure 3 shows the RFS in the high-risk group and intermediate-risk group according to the postoperative radiation. As clearly shown, the prognosis of the patients with high-risk HGMs who were treated by early irradiation was significantly better ($P = 0.019$), whereas there were no significant prognostic differences between early irradiation and deferred irradiation in the intermediate-risk HGMs ($P = 0.34$).

Discussion

Since radical resection of meningioma is widely agreed to cause an improvement of prognosis [11], neurosurgeons always attempt to resect the tumor at the highest possible extent irrespective of histological subtype or tumor location. Although some promising antineoplastic agents, such as trabectedin [12] or histone deacetylase inhibitors [13], are being used in preclinical studies, commonly acceptable chemotherapies for HGMs are currently

Table 2. Cox regression Hazard model on RECURRENCE FREE SURVIVAL in deferred irradiation group.

	Univariate analysis			Multivariate analysis		
Factors	**Hazard ratio**	**95% CI**	**P-value**	**Factors**	**Hazard ratio**	**95% CI**
Age*	1.017	0.988–1.05	0.26			
Gende	Male 0.784	0.333–1.84	0.58			
Location	Not convexity 1.852	0.679–5.05	0.229			
Preoperative KPS (%)	80–100% 0.360	0.153–0.844	0.019	0.421	0.166–1.07	0.069
Tumor size	>6.0 cm 1.551	0.632–3.81	0.338			
Histology	Grade III 4.648	1.74–12.4	0.0022	6.68	1.67–26.8	0.0073
Histology at presentation	transformed 3.16	1.26–7.95	0.0144	4.33	1.02–18.4	0.047
Extent of resection (Simpson grade)	Grade 3–5 3.95	1.58–9.89	0.0034	1.167	0.317–4.30	0.82
MIB-1 labeling index (%) (n = 35)	10–15% 0.975	0.323–2.95	0.96	NA	NA	NA
	>15% 3.683	1.23–11.0	0.020	NA	NA	NA

Abbreviations: CI, confidence interval; KPS, Karnofsky performance status; NA, no assessment.
*continuous variable.
doi:10.1371/journal.pone.0097108.t002

Table 3. Recurrence-risk stratification of high-grade meningioma.

Risk group	Classifiers
High-risk group	1 Grade III malignancy
	2 Transformed histology
Intermediate-risk group	1 Poor preoperative KPS score (less than 70%)
	2 Simpson grade 3–5 resection
	3 High MIB-1 labeling index (more than 15%)
Low-risk group	None of matched above factors

Abbreviation: KPS, Karnofsky performance status.
doi:10.1371/journal.pone.0097108.t003

unavailable. Therefore, radiotherapy remains the sole treatment option after surgical resection of HGMs, and the timing of radiotherapy is of great concern to physicians and has been discussed in several retrospective analyses [2,4,5,6].

There is no doubt that radiotherapy for HGMs is beneficial for controlling tumor recurrence and has demonstrated improvement in patient prognosis [2,4]. However, compared to other malignant brain tumors such as high-grade gliomas and medulloblastomas, the role of radiotherapy for HGMs remains ambiguous. Previously, some studies suggested that patients with atypical meningiomas for whom gross total resection is possible do not necessarily need postoperative radiotherapy [5,6]. In addition, Pearson et al. pointed out that the incidence of atypical meningiomas increased dramatically after 2004 due to the reclassification of WHO criteria [6]. Our series also show this trend, as 39 (71%) out of the 55 cases were diagnosed as HGMs after 2004. This fact might indicate that recent cases diagnosed as HGM might include cases that did not meet the old criteria, suggesting in turn that the number of surgically curable HGMs may have recently increased.

The main aim of this study is to attempt to identify the prognostic risk factors of early recurrence that are available at the time physicians decide whether postoperative irradiation should be performed. To eliminate the influence of radiotherapy, we specifically focused on HGM patients who did not received postoperative radiotherapy at primary HGM diagnosis. Thereafter, we stratified our patient pool into three recurrence-risk groups according to these factors, which were identified by multivariate and univariate analyses, and we validated the survival effect for each of these groups. Although this novel approach is debatable, we propose that it can provide some clues for the treatment strategy of this rare disease.

Through this analysis, we were able to identify two significant risk factors: Grade III malignancy and transformed histology. In terms of Grade III meningioma, previous reports evidently recommended postoperative radiotherapy regardless of the extent of resection [14,15]. Durand et al. evaluated the prognostic factors for high-grade meningioma on 199 adult patients. Although no significant difference was found in overall survival rate between the patients who had and had not received radiation adjuvant treatment, it was found that only the prognosis of Grade III meningioma could be improved by postoperative radiotherapy [16]. These results are consistent with our analysis.

The other significant poor risk factor is transformed malignancy. In our series, all transformed HGM cases ranged from benign to atypical. Nevertheless, the prognosis of these patients was significantly poor, as was that of the Grade III meningioma patients. With respect to glioblastoma, secondary malignancy is representative of a good prognostic factor [17], whereas the malignant transformation exhibited contrasting findings for HGM. This poor prognostic factor was also recognized by two previous

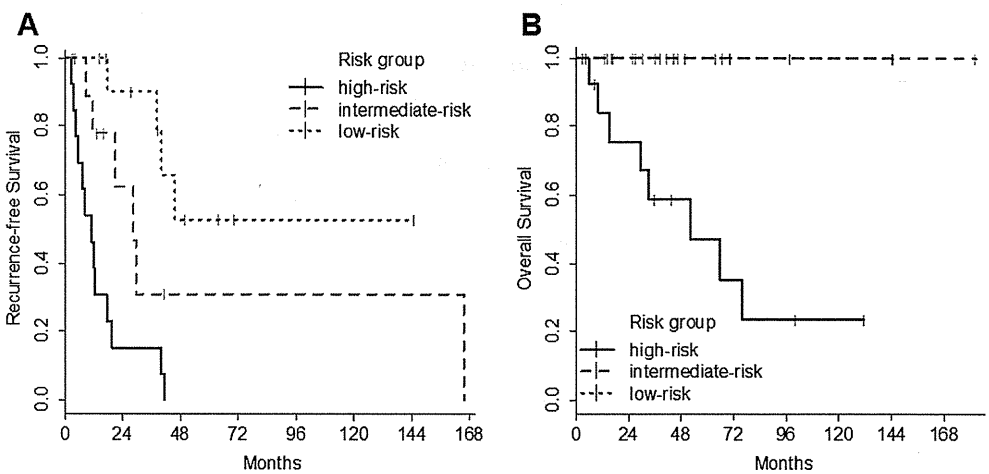

Figure 2. Kaplan-Meier estimates based on the recurrence-risk stratification. The graphs show recurrence-free survival (A) and overall survival (B) according to the recurrence-risk stratification defined as prognostic factors. Prognosis shows a significant difference in both RFS and OS among the recurrence-risk stratified groups ($p<0.001$ in PFS, $P=0.001$ in OS).
doi:10.1371/journal.pone.0097108.g002

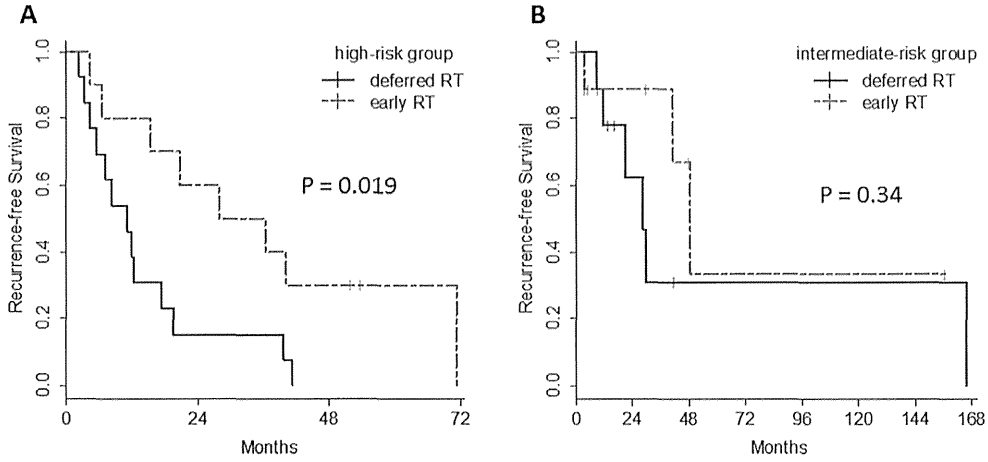

Figure 3. Recurrence-free survival analysis according to postoperative irradiation. Kaplan-Meier estimates of recurrence-free survival are illustrated according to the treatment option of postoperative irradiation in high-risk group (A) and intermediate-risk group (B). In high-risk group, the prognosis of the patients with early irradiation was significantly better (P = 0.019), whereas there were no significant prognostic differences between early irradiation and deferred irradiation in the intermediate-risk HGMs (P = 0.34). RT stands for radiation therapy.
doi:10.1371/journal.pone.0097108.g003

studies [8,18]. Interestingly, Krayenbühl et al. demonstrated the significant differences of histological characters, in addition to cytogenetic findings between "de novo" subgroup and "transformed" subgroup. They hypothesized that the "transformed" HGMs could comprise distinct subgroups of aggressive meningiomas compared to "de novo" HGMs [8]. In addition, Yang et al. reported that tumors with malignant transformation had a higher percentage of p53 overexpression than "de novo" tumors [18]. Their findings are consistent with our results, and can provide the biological clues toward a better understanding of the poor prognosis of this subpopulation.

For the classifiers of the intermediate-risk group, three risk factors were designated based on univariate analyses: patients' poor preoperative KPS, incomplete tumor resection, and tumors with high MIB-1 labeling indices. Our series failed to demonstrate a significant beneficial effect from gross total resection in multivariate analysis, suggesting that the extent of resection is not always a definitive prognostic factor for HGM patients. In addition, we adopted the MIB-1 labeling index as a prognostic factor by histological aspect. It is well known that the MIB-1 labeling index is routinely performed worldwide and recognized as one of the most reliable markers of proliferative tumor activity [19]. Compared to Grade III meningioma, it is commonly recognized that the diagnosis criteria of Grade II meningiomas are highly controversial despite the objective criteria of WHO classification. In actuality, the difference of mean MIB-1 labeling index among the studies was significant, ranging from 3.2%[18] to 15.81% [20]. To complement this interinstitutional or interobserver difference, the "high MIB-1 labeling index" became a proper objective factor to identify the tumors that might pose a potential risk for early recurrence.

For the treatment of high-risk HGM patients, we advocate postoperative radiotherapy regardless of the extent of resection. As shown in Figure 3A, early irradiation could contribute to prolonged recurrence-free survival of the patients with high-risk HGM. On the other hand, patients with low-risk HGMs should not be given up-front radiotherapy. Low-risk HGMs might be curable without irradiation and the patients may ultimately remain free of recurrent disease, as with the patients who undergo complete resection of benign meningiomas. In addition, in the instance that low-risk HGMs relapse, our data suggests that the recurrent tumor could be regulated via salvage operation or radiotherapy. Compared to the high-risk and low-risk groups, the biological behaviors and clinical courses of the intermediate-risk HGMs are heterogeneous. It is ambiguous whether the patients in the intermediate-risk group should receive postoperative radiotherapy. The Kaplan-Meier curves in Fig. 3B provide a visual representation of the recurrence pattern. These curves indicate that the intermediate-risk group included tumors with a high possibility of early recurrence, especially for the first three years following diagnosis, as well as tumors that are potentially curable without irradiation.

Conclusions

Although the influence of irradiation will likely be difficult to fully elucidate in a single-institution series, our scrupulous analysis provides a clue as to how to manage treatment for HGM patients. We propose recurrence-risk stratification using available clinical and histopathological factors for the purpose of making decisions regarding radiotherapy for postoperative HGM patients. Multicenter reviews and prospective studies are necessary to evaluate this stratification system for validity.

Author Contributions

Conceived and designed the experiments: SY ST KH HS. Performed the experiments: HN H. Kanno. Analyzed the data: SY YI. Contributed reagents/materials/analysis tools: ST H. Kobayashi KA HM RO. Wrote the paper: SY ST.

References

1. Claus EB, Bondy ML, Schildkraut JM, Wiemels JL, Wrensch M, et al. (2005) Epidemiology of intracranial meningioma. Neurosurgery 57: 1088–1095.

2. Adeberg S, Hartmann C, Welzel T, Rieken S, Habermehl D, et al. (2012) Long-term outcome after radiotherapy in patients with atypical and malignant

meningiomas—clinical results in 85 patients treated in a single institution leading to optimized guidelines for early radiation therapy. Int J Radiat Oncol Biol Phys 83: 859–864.
3. Pasquier D, Bijmolt S, Veninga T, Rezvoy N, Villa S, et al. (2008) Atypical and malignant meningioma: outcome and prognostic factors in 119 irradiated patients. A multicenter, retrospective study of the Rare Cancer Network. Int J Radiat Oncol Biol Phys 71: 1388–1393.
4. Aghi MK, Carter BS, Cosgrove GR, Ojemann RG, Amin-Hanjani S, et al. (2009) Long-term recurrence rates of atypical meningiomas after gross total resection with or without postoperative adjuvant radiation. Neurosurgery 64: 56–60.
5. Mair R, Morris K, Scott I, Carroll TA (2011) Radiotherapy for atypical meningiomas. J Neurosurg 115: 811–819.
6. Pearson BE, Markert JM, Fisher WS, Guthrie BL, Fiveash JB, et al. (2008) Hitting a moving target: evolution of a treatment paradigm for atypical meningiomas amid changing diagnostic criteria. Neurosurg Focus 24: E3.
7. Motegi H, Kobayashi H, Terasaka S, Ishii N, Ito M, et al. (2012) Hemorrhagic onset of rhabdoid meningioma after initiating treatment for infertility. Brain Tumor Pathol 29: 240–244.
8. Krayenbuhl N, Pravdenkova S, Al-Mefty O (2007) De novo versus transformed atypical and anaplastic meningiomas: comparisons of clinical course, cytogenetics, cytokinetics, and outcome. Neurosurgery 61: 495–503.
9. Simpson D (1957) The recurrence of intracranial meningiomas after surgical treatment. J Neurol Neurosurg Psychiatry 20: 22–39.
10. Kanno H, Nishihara H, Wang L, Yuzawa S, Kobayashi H, et al. (2013) Expression of CD163 prevents apoptosis through the production of granulocyte colony-stimulating factor in meningioma. Neuro Oncol 15: 853–864.
11. Palma L, Celli P, Franco C, Cervoni L, Cantore G (1997) Long-term prognosis for atypical and malignant meningiomas: a study of 71 surgical cases. J Neurosurg 86: 793–800.
12. Preusser M, Spiegl-Kreinecker S, Lotsch D, Wohrer A, Schmook M, et al. (2012) Trabectedin has promising antineoplastic activity in high-grade meningioma. Cancer 118: 5038–5049.
13. Bush ML, Oblinger J, Brendel V, Santarelli G, Huang J, et al. (2011) AR42, a novel histone deacetylase inhibitor, as a potential therapy for vestibular schwannomas and meningiomas. Neuro Oncol 13: 983–999.
14. Dziuk TW, Woo S, Butler EB, Thornby J, Grossman R, et al. (1998) Malignant meningioma: an indication for initial aggressive surgery and adjuvant radiotherapy. J Neurooncol 37: 177–188.
15. Rosenberg LA, Prayson RA, Lee J, Reddy C, Chao ST, et al. (2009) Long-term experience with World Health Organization grade III (malignant) meningiomas at a single institution. Int J Radiat Oncol Biol Phys 74: 427–432.
16. Durand A, Labrousse F, Jouvet A, Bauchet L, Kalamarides M, et al. (2009) WHO grade II and III meningiomas: a study of prognostic factors. J Neurooncol 95: 367–375.
17. Ohgaki H, Dessen P, Jourde B, Horstmann S, Nishikawa T, et al. (2004) Genetic pathways to glioblastoma: a population-based study. Cancer Res 64: 6892–6899.
18. Yang SY, Park CK, Park SH, Kim DG, Chung YS, et al. (2008) Atypical and anaplastic meningiomas: prognostic implications of clinicopathological features. J Neurol Neurosurg Psychiatry 79: 574–580.
19. Perry A, Stafford SL, Scheithauer BW, Suman VJ, Lohse CM (1998) The prognostic significance of MIB-1, p53, and DNA flow cytometry in completely resected primary meningiomas. Cancer 82: 2262–2269.
20. Ko KW, Nam DH, Kong DS, Lee JI, Park K, et al. (2007) Relationship between malignant subtypes of meningioma and clinical outcome. J Clin Neurosci 14: 747–753.

Acta Neurochir
DOI 10.1007/s00701-014-2290-7

CLINICAL ARTICLE - BRAIN TUMORS

Combined use of 18 F-FDG PET and corticosteroid for diagnosis of deep-seated primary central nervous system lymphoma without histopathological confirmation

Shigeru Yamaguchi · Kenji Hirata · Sadahiro Kaneko · Hiroyuki Kobayashi · Tohru Shiga · Kentaro Kobayashi · Rikiya Onimaru · Hiroki Shirato · Nagara Tamaki · Shunsuke Terasaka · Kiyohiro Houkin

Received: 23 September 2014 / Accepted: 20 November 2014

Abstract
Background Although histological diagnosis is indispensable in treating primary central nervous system lymphoma (PCNSL), we sometimes face an intractable situation in which tissue can be obtained only from a deep-seated brain lesion. In place of a histological diagnosis, the diagnostic adequacy of the combined use of 18 F-FDG PET and corticosteroid administration for PCNSL located in a deep-seated brain structure is reported.
Methods Patients with a deep-seated tumor were treated as having PCNSL without histological confirmation, based on the following criteria: (1) there was no evidence of systemic malignancy; (2) the tumor showed an extremely high FDG uptake relative to normal gray matter on pretreatment 18 F-FDG PET; (3) the tumor decreased in size 1 week after diagnostic therapy by corticosteroid administration on contrast-enhanced T1-weighted magnetic resonance imaging (MRI). FDG uptake of the lesion was evaluated by the maximum of standardized uptake values (SUVmax) and tumor-to-normal ratio of the SUV (T/N ratio). The extent of the tumor reduction was calculated by volumetric analysis for the treatment response to corticosteroid administration.
Results Ten patients (4 males and 6 females) matched these criteria. On pretreatment 18 F-FDG PET, mean SUVmax in the tumor was 24.8 (8.75–60.75), and mean T/N ratio was 3.24 (2.17–5.12). The extent of tumor volume reduction was shown to be 21 to 68 % 1 week after diagnostic therapy by corticosteroids. Mean total dose and duration of corticosteroids were 719 mg as prednisolone and 6.5 days, respectively. Nine patients achieved complete response and one patient achieved partial response on MRI after standard treatment for PCNSL with high-dose methotrexate and/or whole-brain irradiation.
Conclusion Although the value of biopsy is universal, combining 18 F-FDG PET and corticosteroid administration is an important alternative method that may lead to the diagnosis of deep-seated PCNSLs in cases with intractable histopathological confirmations.

Keywords Brain tumor · Corticosteroid · 18 F-FDG · Position emission tomography · Primary central nervous system lymphoma

Introduction

Tumor resection has not contributed to the treatment of the primary central nervous system lymphoma (PNCSL) because it has not been associated with any survival benefits and in fact may lead to neurological deficits resulting from treatment delays [14]. In addition, since almost all PCNSLs are diffuse large B-cell lymphomas, the treatment strategy is rarely changed by subtype. Nevertheless, histological diagnosis should be performed before any adjuvant treatment for PCNSL, since the adjuvant treatment strategy is quite different from that of other malignant brain tumors, such as high-grade

S. Yamaguchi · S. Kaneko · H. Kobayashi · S. Terasaka (✉) · K. Houkin
Department of Neurosurgery, Graduate School of Medicine, Hokkaido University, 5 West 7, Kita-ku, 060-8638 Sapporo, Japan
e-mail: terasas@med.hokudai.ac.jp

K. Hirata · T. Shiga · K. Kobayashi · N. Tamaki
Department of Neurosurgery, Nuclear Medicine, Graduate School of Medicine, Hokkaido University, Sapporo, Japan

R. Onimaru · H. Shirato
Department of Neurosurgery, Radiation Oncology, Graduate School of Medicine, Hokkaido University, Sapporo, Japan

Published online: 10 December 2014

gliomas or metastatic brain tumors. However, difficult biopsies are occasionally encountered, particularly when the tumor is located in a deep-seated region and in other critical brain structures, such as the hypothalamus and the brain stem.

Magnetic resonance imaging (MRI) is routinely performed upon diagnosis of PCNSL. The MRI features of PCNSL are well recognized by relatively characteristic features, i.e., they display contrast enhancement and no necrosis [19]. However, MRI appearances of high-grade gliomas or inflammatory disorders sometimes mimic that of PCNSLs. Thus, the MRI appearance alone cannot confirm the diagnosis. On the other hand, the usefulness of 18 F-FDG (FDG) PET on PCNSLs has been reported, and an FDG PET appearance could play a subsidiary role in the diagnosis of PCNSLs [2, 15, 16, 18]. PCNSLs usually show an extremely high FDG uptake compared to other brain tumors, and we demonstrated that the tumor-to-normal brain uptake ratio (T/N ratio) is the appropriate parameter for distinguishing PCNSL from other malignant intraaxial brain tumors [18].

In addition, PCNSLs are known to be exquisitely sensitive to the lympholytic effect of corticosteroids [10]. There are anecdotal reports of the complete radiological disappearance of tumors and survival for more than a year with steroids alone [4]. It is also known that these agents may result in a complete radiographic response or even an uninformative pathological biopsy [2].

With this in mind, we report a total of ten PCNSL cases in which tissue biopsies were not taken and yet the patients were successfully treated with high-dose methotrexate (HDMTX) and/or whole-brain irradiation after diagnosis based on MRI, FDG PET, and the response to corticosteroid administration. We use these cases to present acceptable criteria for diagnosis by using both FDG PET and corticosteroid administration for PCNSLs.

Patients and methods

Patients

This study was performed with the approval of the Internal Review Board on Ethical Issues of Hokkaido University Hospital, Sapporo, Japan (no. 014-0142). Patients with intractable histological confirmation by biopsy were treated as having PCNSL after fulfilling the following criteria: (1) there was no evidence of systemic malignancy; (2) the tumor was located in a deep site of the brain, such as in the hypothalamus (Fig. 1a), brainstem including the cerebral peduncle (Fig. 1b), and cerebellar peduncle (Fig. 1c), or periventricular infiltration (Fig. 1d); (3) the tumor had a high FDG uptake on PET, which is defined as when the FDG uptake of the lesion is relatively higher than that of the adjacent and contralateral gray matter based on the visual inspection (Fig. 1); (4) patients were radiological responders to corticosteroid administration, which is described in detail below. Written informed consent was obtained from all of the patients included in this report.

A chemotherapy regimen of three cycles of HDMTX (3.5 g/m^2 as an intravenous rapid infusion in 3 h) on the first day of a 14-day cycle was applied in the usual fashion. After completion of chemotherapy, whole-brain irradiation was given to a total dose of 30–40 Gy in 15–20 fractions of 2 Gy given daily on weekdays with or without a tumor bed boost. The patients who could not tolerate HDMTX only underwent whole-brain irradiation with a tumor bed boost.

MR imaging and volumetric analysis

The MR imaging evaluation included routine conventional multiplanar brain scans at a field strength of 1.5 T with and without gadolinium contrast. Quadrature head coils on four different GE MRI scanners were used (GE Health Care, Milwaukee, WI). In addition to routine T1-weighted images (T1WI), T2-weighted images (T2WI), fluid-attenuated inversion recovery (FLAIR) and gradient echo sequences, echo planar diffusion-weighted images (DWI) (b=1,000s/mm^2) were obtained. Using in-house software based on DICOM data, manual segmentation was performed with region-of-interest analysis to measure tumor volumes on the basis of contrast-enhanced T1WI axial slices. The extent of tumor volume reduction by steroid administration was calculated as ((pre-treatment tumor volume)—(tumor volume after steroid administration))/(pre-treatment tumor volume).

PET protocol and imaging analysis

Detailed PET protocol and imaging analysis has been described previously [18]. Briefly, following a blood glucose test excluding hyperglycemia, a 4.5 MBq/kg of FDG was intravenously injected, and the whole brain was scanned 1 h later. All the images were acquired using a high-resolution PET scanner (ECAT HR+ scanner; Asahi-Siemens Medical Technologies Ltd., Tokyo, Japan) operated in a three-dimensional mode or scanned using an integrated PET-CT scanner (Biograph 64 PET-CT scanner; Asahi-Siemens Medical Technologies Ltd., Tokyo, Japan). Attenuation-corrected radioactivity images for both scanners were reconstructed using ordered subset expectation maximization with a Hann filter of 4 mm full width half maximum.

A circular region of interest, 10 mm in diameter, was placed in the lesion at the area corresponding to the MRI abnormality. Regional uptake of FDG was expressed as a standardized uptake value (SUV) calculated as (tissue activity [Bq/ml]) × (body weight [g])/(injected radioisotope activity [Bq]). Maximum SUV (SUVmax) of tumors was sampled from the single pixel showing the highest FDG accumulation. The T/N ratio was defined as the ratio of the SUVmax of the

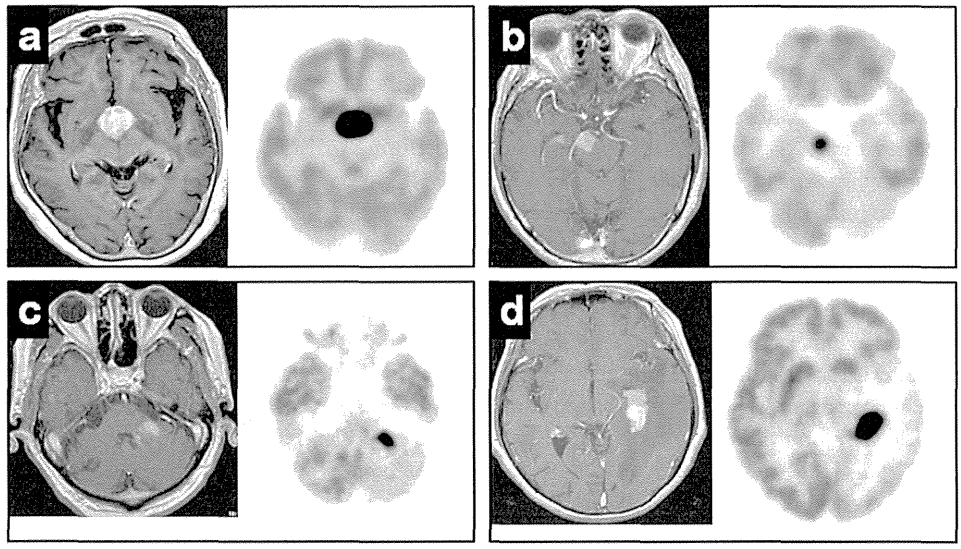

Fig. 1 Representative magnetic resonance imaging (MRI) and FDG-PET findings of deep-seated primary central nervous system lymphoma located in the hypothalamus (**a**), cerebral peduncle (**b**), cerebellar peduncle (**c**), and periventricular infiltration (**d**)

lesion to the SUVmax of the contralateral normal gray matter on the same axial plane. For the central lesion, the average SUVmax of both sides of the gray matter were adopted as the normal SUV.

Assessment of steroid response

After completing the imaging studies, corticosteroid was administered to every patient. Duration and cumulative total dose of steroid therapy depend on the patient's age and associated diseases. Cumulative corticosteroid dose was calculated by conversion to prednisolone. MRI with contrast enhancement was performed approximately 1 week after corticosteroid administration. The treatment response was assessed by the patient condition and MRI findings. The patient condition was assessed by the Karnofsky Performance Status (KPS). For the radiological response evaluation, the volume of the contrast enhancement lesion on MRI was compared before and after corticosteroid administration, as described above.

Results

Patient characteristics

We retrospectively identified 10 patients, 4 male and 6 female (age range 46–80 years; mean 69.6) who matched the criteria described above and were treated by HDMTX and/or radiation therapy as having PCNSL without histological confirmation since 2007 (Table 1). The lesions were located in the hypothalamus in four patients, cerebral peduncle in one, cerebellar peduncle in two, and periventricular infiltration in four. One patient (case 4) suffered from multiple lesions located in the hypothalamus and periventricular infiltration, and two patients (cases 2 and 6) suffered from tumor spreading into the bilateral ventricular walls.

Six patients developed consciousness disturbance due to direct tumor invasion. In addition, two patients showed intratumoral hemorrhage at presentation (case 5, Fig. 2a; case 6, Fig. 2b). Median KPS of ten patients at admission was quite low at 40.

Screening body CT was performed on all patients, and bone marrow biopsy was performed on nine out of ten patients. In addition, six patients underwent whole-body FDG PET scans simultaneously with a first-time brain FDG PET. There was no evidence of systemic lymphoma throughout these examinations for any of the patients. Serum soluble interleukin-2 receptor (sIL-2R) was also investigated in all patients on admission, and slight elevation of the serum level of sIL-2R was observed in two cases (cases 4 and 8) compared to age-matched healthy controls. By ophthalmological examination, vitreous opacity was strongly suspected in two cases (cases 7 and 9), but definitive diagnostic procedures could not be performed because of poor patient condition. In the MRI, all lesions were demonstrated via contrast enhancement with marked cerebral edema. Increased diffusivity of water protons was displayed in all patients, except one with massive intratumoral hemorrhage (case 6).

FDG PET appearance and response to corticosteroid administration

The lesions were visually detected as high uptake compared to adjacent and contralateral gray matter on pretreatment FDG PET. SUVmax of FDG uptake in the tumor ranged from 8.75 to 60.57, with a mean of 24.83. The T/N ratio in the tumor ranged from 2.17 to 5.12, with a mean of 3.24 (Table 1).

Table 1 Individual characteristics of the deep-seated primary central nervous system lymphoma (PCNSL) without pathological confirmation

Case no.	Age/ sex	Tumor location	FDG PET	Status at onset			Status after steroid administration			Curative therapy	Status after curative therapy		Follow-up	
			SUV max	T/N ratio	KPS (%)	Tumor volume (ml)	KPS (%)	Tumor volume (ml)	Extent of reduction (%)		Response	KPS (%)	Months	Status
1	79/F	CeP	15.35	2.60	40	6.84	40	2.22	68 %	HDMTX + RT	CR	40	25	PD
2	55/F	PV	43.3	3.12	40	13.91	50	8.38	40 %	HDMTX + RT	CR	100	36	CR
3	74/F	PV	13.74	2.17	70	10.54	80	5.51	48 %	HDMTX + RT	CR	100	43	CR
4	69/F	PV and HT	21.86	3.64	30	17.71	50	8.76	51 %	HDMT + RT	CR	70	3[a]	CR
5	74/F	HT	33.8	2.77	30	7.07	40	2.40	66 %	HDMTX + RT	CR	60	8	D
6	46/M	PV	8.75	2.60	30	N/A	60	N/A	N/A	HDMTX + RT	CR	90	29	CR
7	70/M	CeP	14.66	2.81	50	1.85	50	0.89	52 %	HDMTX + RT	CR	60	21	CR
8	75/M	HT	14.01	2.50	40	7.40	50	2.59	65 %	RT	CR	50	6	D
9	74/F	HT	60.57	5.06	50	6.05	50	4.76	21 %	RT	PR	50	5	D
10	80/M	CP	22.22	5.12	50	1.97	60	0.80	59 %	RT	CR	70	13	CR

CP cerebral peduncle; *CeP* cerebellar peduncle; *CR* complete response; *D* dead; *HDMTX* high-dose methotrexate chemotherapy; *HT* hypothalamus; *KPS* Karnofsky Performance Status; *N/A* not applicable; *PD* progressive disease; *PR* partial response; *PV* periventricular infiltration; *RT* radiation therapy; *SUVmax* maximum of standardized uptake value; *T/N ratio* tumor-to-normal SUV ratio

[a] Lost to follow-up after curative chemo-radiotherapy

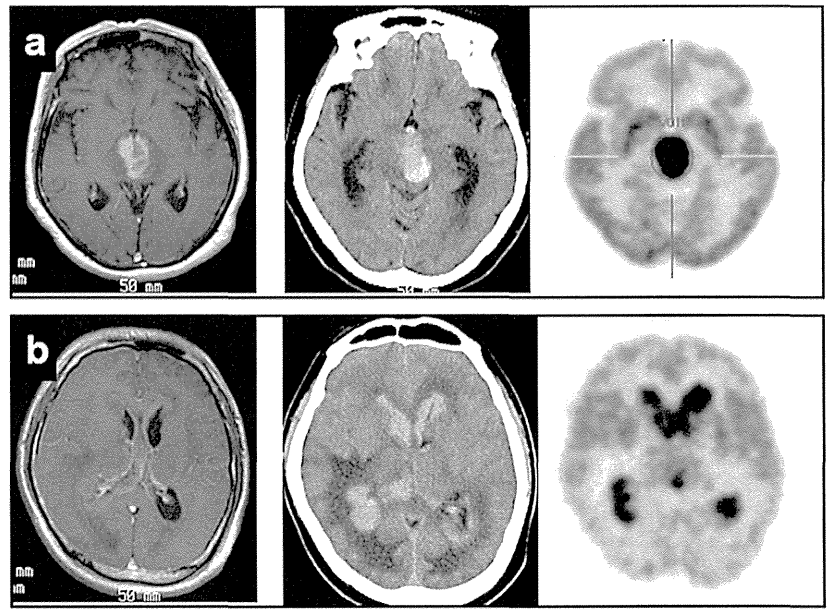

Fig. 2 Two deep-seated PCNSL cases presented with intratumoral hemorrhage: case 5 (**a**); case 6 (**b**)

Corticosteroid administration began within 3 days after admission for all patients. Total amount of applied corticosteroid (as prednisolone) ranged from 200 to 2,400 mg (mean, 719 mg), and duration of administration ranged from 3 to 10 days (mean, 6.5 days). The patients' conditions were improved in seven out of ten cases. All patients showed a radiological response to steroid administration, and the extent of tumor volume reduction was shown to be 21 to 68 % (Table 1, Fig. 3).

Treatments and outcomes

Seven patients received chemotherapy with HDMTX. Six out of seven patients could achieve three cycles, but one of them underwent only two cycles because of poor responsiveness to HDMTX. These patients were treated with whole-brain irradiation after HDMTX. The tumor bed boost with 10 Gy was given to five patients. Three patients could not undergo HDMTX mainly because of poor renal function; therefore, these patients received whole-brain irradiation with a tumor bed boost.

All treatments were well tolerated, and there were no severe adverse episodes. Nine patients achieved a complete response (CR), and one patient achieved a partial response (PR) on MRI at the end of radiation therapy. The median KPS after treatment remarkably improved up to 65 (range from 40 to 100). Although one patient (case 4) was lost to follow-up just after discharge from our hospital, nine patients could be followed up after curative chemo-radiotherapy. Three out of nine patients died because of the tumor within 1 year, whereas five out of nine patients remained clinically and radiologically stable without tumor relapse at the end of follow-up (Table 1).

Representative case

Case 2 (Fig. 4)

A 55-year-old female ultimately became stuporous and was referred to our institute. The MRI showed contrast-enhancing lesions along the whole ventricular system. The T2-weighted image exhibited signal abnormality, especially in the bilateral parieto-occipital periventricular white matter. MRI findings indicate PCNSL (Fig. 4a-c). The results of the chest and abdominal CT as well as the bone marrow biopsy showed no evidence of systemic lymphoma. Human immunodeficiency virus testing, CSF studies, and ophthalmological examination showed no abnormality.

The patient underwent FDG PET following our protocol and obtained a SUVmax of 43.3 and T/N ratio of 3.12, respectively (Fig. 4d). Prednisolone at a total of 1,300 mg had been administrated intravenously for 4 days. Her consciousness improved 5 days after steroid administration, and the MRI showed a remarkable reduction in the enhanced lesions (Figs. 3 and 4). Based on the MRI, FDG PET findings, and response to steroid administration, the patient was diagnosed with PCNSL.

She received three cycles of chemotherapy with HDMTX (3.5 g/m^2) with no severe adverse events. Whole-brain irradiation was given to a total dose of 30 Gy in 15 fractions of 2 Gy

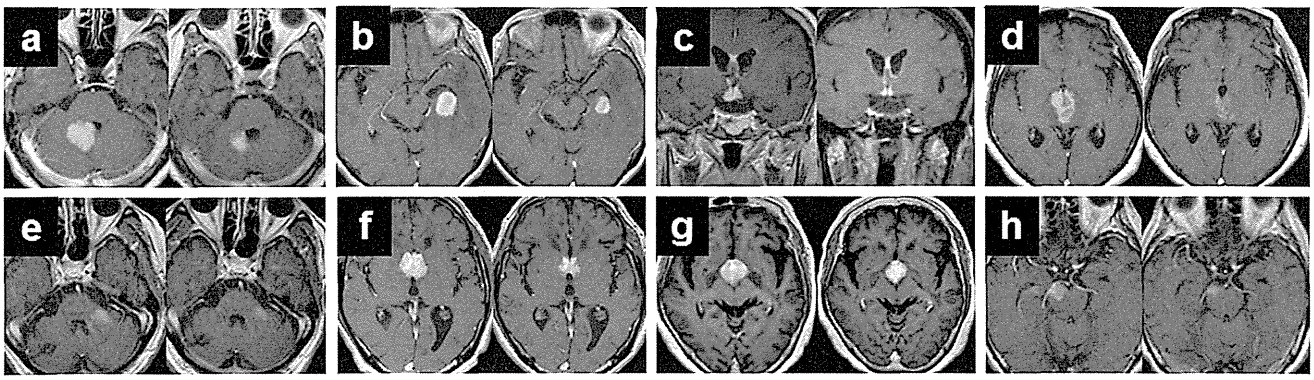

Fig. 3 Contrast-enhanced MRI appearances of pre- (left) and post-corticosteroid (right) administration. (**a**)-(**h**) correspond to cases 1, 3, 4, 5, 7, 8, 9, and 10, respectively. Case 2 is presented in Fig. 4 as a representative case. Case 6 is not presented because no assessable contrast-enhanced lesion could be observed because of massive intratumoral hemorrhage, as shown in Fig. 2b

given daily on weekdays without a tumor bed boost. She achieved complete response (CR) on the MRI after treatment and returned to normal life (Fig. 4f). She has stayed well for 3 years without any evidence of lesions on MRI.

Discussion

Deep-seated primary central nervous system lymphoma

Image-guided stereotactic biopsy is the chosen method for histopathological diagnosis for PCNSL because gross tumor resection is not recommended [14]. However, this procedure is considerably difficult in the following situations: (1) when the patient is in poor general condition and cannot tolerate surgery, (2) when the lesion has a potential risk for non-diagnostic biopsy, or (3) when the lesion is deep seated or adjacent to vital structures with a risk of surgical complication. Our ten reported cases correspond to these situations. In addition, since two patients had lesions with fresh hemorrhage at onset, the biopsy procedure itself had significant risk of additional bleeding and could have led to a worse condition.

Stereotactic biopsy has generally been regarded as a safe procedure; however, Kongkham et al. reported 4.8 % symptomatic intracranial hemorrhage in 622 cases of frame-based stereotactic biopsy [7]. They also stated that the subgroup with deep-seated lesions may have an elevated risk of overall complications. Although there are a few papers concerning nondiagnostic biopsy or biopsy failure, hard tumors, lesions

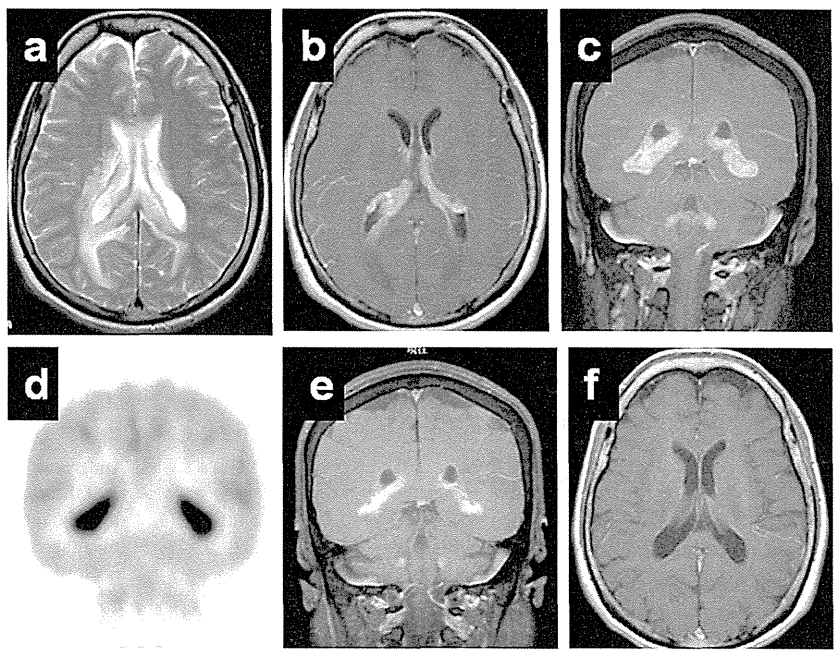

Fig. 4 Representative case presentation (case 2). (**a**) T2-weighted image shows signal abnormality in bilateral parieto-occipital periventricular white matter. (**b, c**) Contrast-enhanced T1-weighted imaging shows contrast-enhancing lesions along the whole ventricular system. (**d**) The patient obtained a SUVmax of 43.3 and T/N ratio of 3.12, respectively. (**e**) MRI showed remarkable reduction in the enhanced lesion after corticosteroid application. (**f**) The patient reached complete response after three courses of HDMTX and whole-brain irradiation

adjacent to the ventricles, and inaccurate tissue sampling were suggested as possible explanations [5].

Imaging modalities for PCNSL diagnosis

MRI is the best imaging modality for assessing PCNSL. Previously reported imaging features of PCNSL are contrast-enhancing lesions with a diameter of at least 15 mm in contact with the subarachnoid space [8]. The mass effect of PCNSL is mostly attributed to the edema and not to the lesion itself. The extent of the edema does not depend on the lesion localization. Necrosis is a rare finding and does not correlate with lesion size. The most frequent locations of PCNSL were the cerebral hemispheres, followed by the basal ganglia and thalamus. Mass lesions originating from the ventricular walls and choroid plexus extending into the ventricular lumen are about 10 % of the lesion. These lesions are not associated with hydrocephalus, but with the cerebral edema of the adjacent cerebral tissue [8]. With a better understanding of these characteristic MRI features of PCNSL, the diagnosis of PCNSL can be inferred in most cases. Conversely, in the absence of typical features of glioblastoma (GBM), i.e., a GBM with relatively homogeneous enhancement, tumefactive enhancing lesions such as those in multiple sclerosis, neurosarcoidosis, and toxoplasmosis pose significant diagnostic challenges [13].

Clinical studies in non-Hodgkin lymphoma (NHL) suggest that FDG PET may be superior to anatomic-based imaging, such as CT and MRI, in assessing residual abnormal lesions following initial therapy [17]. Mohile et al. reported the results of FDG PET imaging with 12 PCNSL patients. In their report, all patients who received prior steroid therapy and suffered from intratumoral hemorrhage showed hypermetabolic lesions with a median SUV of 15 [11]. Karantanis et al. reported that the sensitivity of FDG PET/CT in detecting active PCNSL in the brain was 87 %. Limited to patients with initial staging, all had positive PET findings [6]. Makino et al. demonstrated that the addition of the SUVmax of FDG PET improved the differentiation between PCNSL and GBM [9]. We recently reported that the T/N ratio was superior to the SUVmax in terms of distinguishing PCNSLs from other malignant brain tumors, and optimal cutoff values were 2.0 [18]. All ten cases in the current report had T/N ratios above 2.0, suggesting that the FDG PET findings strongly supported the diagnosis of PCNSL.

Response to corticosteroid administration

In addition to the FDG PET appearance, we attach importance to the response to steroid administration. The total dose and duration of applied corticosteroid optimal for assessing radiological responders was not evident [10]. In general, anti-edema and cytotoxic effects by corticosteroid appeared dramatically in the short term and resulted in improvement of neurological performance and mass shrinking in PCNSL patients. Indeed, malignant gliomas have also been known to lose contrast enhancement with corticosteroid administration [20], but the beneficial effect of corticosteroid is thought to be due to a decrease in the extent of peritumoral edema [1]. MRIs performed approximately a week after steroid administration showed radiological response in all ten patients, and the mean total dose and duration of steroids were 719 mg as prednisolone and 6.4 days, respectively.

Tumefactive enhancing lesions, multiple sclerosis, and toxoplasmosis could be diagnosed by findings of the FDG PET. Only neurosarcoidosis is radiologically difficult to distinguish from PCNSL because of similar MRI and FDG PET findings [3]. A greater 18 F-FDG than ^{11}C-methionine uptake was reported as a marker for its diagnosis [12].

Finally, it is quite important that suspected patients with deep-seated PCNSL should not be treated by corticosteroids before FDG PET examination when we are going to apply this diagnostic procedure. Since FDG uptake of PCNSL may be reduced by corticosteroid administration [18], the diagnostic accuracy of this procedure might decrease. We have to keep in mind that we should examine the treatment history of the patient before FDG PET examination.

Conclusion

By adding FDG PET and corticosteroid administration to conventional MRI, patients unable to receive histopathological confirmation could be presumed to have PCNSL and thus receive appropriate treatment. Although the value of biopsy is universal, characteristic MRI features, hypermetabolism on FDG-PET, and good radiological response to corticosteroid administration are important clinical tools leading to the diagnosis of PCNSL.

Conflicts of interest

None.

References

1. Andersen C, Haselgrove JC, Doenstrup S, Astrup J, Gyldensted C (1993) Resorption of peritumoural oedema in cerebral gliomas during dexamethasone treatment evaluated by NMR relaxation time imaging. Acta Neurochir (Wien) 122:218–224
2. Baraniskin A, Deckert M, Schulte-Altedorneburg G, Schlegel U, Schroers R (2011) Current strategies in the diagnosis of diffuse large B-cell lymphoma of the central nervous system. Br J Haematol 156: 421–432

3. Bolat S, Berding G, Dengler R, Stangel M, Trebst C (2009) Fluorodeoxyglucose positron emission tomography (FDG-PET) is useful in the diagnosis of neurosarcoidosis. J Neurol Sci 287:257–259
4. Bromberg JE, Siemers MD, Taphoorn MJ (2002) Is a "vanishing tumor" always a lymphoma. Neurology 59:762–764
5. Hall WA (1998) The safety and efficacy of stereotactic biopsy for intracranial lesions. Cancer 82:1749–1755
6. Karantanis D, O'Eill BP, Subramaniam RM, Witte RJ, Mullan BP, Nathan MA, Lowe VJ, Peller PJ, Wiseman GA (2007) 18F-FDG PET/CT in primary central nervous system lymphoma in HIV-negative patients. Nucl Med Commun 28:834–841
7. Kongkham PN, Knifed E, Tamber MS, Bernstein M (2008) Complications in 622 cases of frame-based stereotactic biopsy, a decreasing procedure. Can J Neurol Sci 35:79–84
8. Kuker W, Nagele T, Korfel A, Heckl S, Thiel E, Bamberg M, Weller M, Herrlinger U (2005) Primary central nervous system lymphomas (PCNSL): MRI features at presentation in 100 patients. J Neurooncol 72:169–177
9. Makino K, Hirai T, Nakamura H, Murakami R, Kitajima M, Shigematsu Y, Nakashima R, Shiraishi S, Uetani H, Iwashita K, Akter M, Yamashita Y, Kuratsu J (2011) Does adding FDG-PET to MRI improve the differentiation between primary cerebral lymphoma and glioblastoma? Observer performance study. Ann Nucl Med 25:432–438
10. Mathew BS, Carson KA, Grossman SA (2006) Initial response to glucocorticoids. Cancer 106:383–387
11. Mohile NA, Deangelis LM, Abrey LE (2008) Utility of brain FDG-PET in primary CNS lymphoma. Clin Adv Hematol Oncol 6(818–820):840
12. Ng D, Jacobs M, Mantil J (2006) Combined C-11 methionine and F-18 FDG PET imaging in a case of neurosarcoidosis. Clin Nucl Med 31:373–375
13. Omuro AM, Leite CC, Mokhtari K, Delattre JY (2006) Pitfalls in the diagnosis of brain tumours. Lancet Neurol 5:937–948
14. Reni M, Ferreri AJ, Garancini MP, Villa E (1997) Therapeutic management of primary central nervous system lymphoma in immunocompetent patients: results of a critical review of the literature. Ann Oncol 8:227–234
15. Roelcke U, Leenders KL (1999) Positron emission tomography in patients with primary CNS lymphomas. J Neurooncol 43:231–236
16. Rosenfeld SS, Hoffman JM, Coleman RE, Glantz MJ, Hanson MW, Schold SC (1992) Studies of primary central nervous system lymphoma with fluorine-18-fluorodeoxyglucose positron emission tomography. J Nucl Med 33:532–536
17. Spaepen K, Stroobants S, Verhoef G, Mortelmans L (2003) Positron emission tomography with [(18)F]FDG for therapy response monitoring in lymphoma patients. Eur J Nucl Med Mol Imaging 30(Suppl 1):S97–105
18. Yamaguchi S, Hirata K, Kobayashi H, Shiga T, Manabe O, Kobayashi K, Motegi H, Terasaka S, Houkin K (2014) The diagnostic role of (18)F-FDG PET for primary central nervous system lymphoma. Ann Nucl Med 28:603–609
19. Zacharia TT, Law M, Naidich TP, Leeds NE (2008) Central nervous system lymphoma characterization by diffusion-weighted imaging and MR spectroscopy. J Neuroimaging 18:411–417
20. Zaki HS, Jenkinson MD, Du Plessis DG, Smith T, Rainov NG (2004) Vanishing contrast enhancement in malignant glioma after corticosteroid treatment. Acta Neurochir (Wien) 146:841–845

Clinical Benefit of ^{11}C Methionine PET Imaging as a Planning Modality for Radiosurgery of Previously Irradiated Recurrent Brain Metastases

Toshiya Momose, MD, Tadashi Nariai, MD, PhD,* Takuya Kawabe, MD,† Motoki Inaji, MD, PhD,* Yoji Tanaka, MD, PhD,* Shinya Watanabe, MD,† Taketoshi Maehara, MD, PhD,* Keiichi Oda, PhD,‡ Kenji Ishii, MD, PhD,‡ Kiichi Ishiwata, PhD,‡ and Masaaki Yamamoto, MD, PhD†§*

Object: Stereotactic radiosurgery with gamma knife (GK-SRS) generally improves the focal control of brain metastases. Yet in cases of focal recurrence at a previous radiation site, MRI is often imperfect in differentiating between active tumor and radiation injury. We have examined whether the use of ^{11}C methionine (MET) with PET will facilitate this differentiation and improve the outcome of GK-SRS for focally recurrent brain metastases after prior treatment.

Methods: Eighty-eight patients underwent GK-SRS for postirradiation recurrent brain metastases. Thirty-four patients received radiation in areas manifesting high MET uptake (PET group) in a dose-planning procedure using MET-PET/MRI fusion images. Fifty-four patients referred from other institutes received radiation based on dose planning information obtained from MRI (MRI group).

Results: Sex, age, and the ratio of breast cancer differed significantly between the MRI and PET groups. The total irradiation volume was significantly smaller in the PET group, and the minimal irradiation dose was significantly higher. In a multivariable statistical analysis, the use of MET-PET ($P = 0.02$) was independently associated with prolonged overall survival after treatment, Karnofsky performance status ($P = 0.002$), the number of lesions ($P = 0.03$), and patient's sex ($P = 0.02$). The median survival time was significantly longer in the PET group (18.1 months) than in the MRI group (8.6 months) ($P = 0.01$).

Conclusion: ^{11}C methionine-PET/MRI fusion images for dose planning lengthened survival in patients undergoing GK-SRS for focally recurrent brain metastases.

Key Words: methionine, PET, recurrent brain metastases, radiosurgery

(*Clin Nucl Med* 2014;39: 939–943)

Gamma knife stereotactic radiosurgery (GK-SRS) is widely acknowledged to be effective for the treatment of newly diagnosed metastatic brain tumors.[1–3] Gamma knife stereotactic radiosurgery may also be helpful when tumors recur focally at or within previous radiation sites or when patients otherwise require additional treatment.[4–7] Yet it can be difficult to differentiate between a recurrent tumor and radiation injury caused by the initial SRS, as necrotic inflammation and recurrent active tumors are both similarly enhanced in gadolinium (Gd) contrast MRI.[8–11]

The authors have long been using ^{11}C methionine (MET) images with PET for the treatment of gliomas.[12] In more recent years, PET-MRI fusion images for surgical navigation have proven to be useful for achieving maximal resection of gliomas and prolonging patients' survival.[12–14] This trend, together with the established use of MET-PET for differentiating active metastatic brain tumor and radiation necrosis, suggests that the same type of approach (ie, MET-PET/MRI fusion images) may facilitate the GK-SRS procedure for locally recurrent brain metastases.[15,16] Our group started using PET-MRI fusion images in GK-SRS interventions for patients treated under our PET program in 2005. In this study, we retrospectively compared the posttreatment survival of these patients with that of patients treated in the same GK center using MRI information alone.

PATIENTS AND METHODS

Patient Population

This was an institutional review board–approved retrospective cohort study (Tokyo Women's Medical University and Tokyo Medical and Dental University). The subjects were selected from among 2502 patients with brain metastases who underwent GK-SRS at Katsuta Hospital Mito Gamma House (our GK center) from 1998 to 2011. Local recurrence at the previously irradiated site, with or without new lesions, was detected in 134 (5.4%) of the patients. Patients with a low Karnofsky performance status (KPS) score due to systemic disease, impaired neurocognitive function (resulting in a noncooperative state), meningeal dissemination, and/or an expected survival period of 3 months or less were excluded from re-treatment (n = 46). The other 88 patients underwent a second GK-SRS. The patients referred from Tokyo Medical and Dental University were enrolled in a PET program and treated using PET-MRI fusion images (n = 34, PET group). The patients referred from the other institutes were treated with MRI information alone (n = 54, MRI group). The patients' characteristics and the overall survival of the 2 groups were statistically compared.

PET Measurements

The PET images were obtained at the PET Center in the Tokyo Metropolitan Institute of Gerontology. The equilibrated radioactivity was measured with a PET scanner (SET 2400 W; Shimadzu, Kyoto, Japan) 20 minutes after administering an intravenous injection of MET (250–300 MBq). Transmission data were acquired in each patient using a rotating 68Ge rod source for attenuation correction. The regional MET uptake was expressed as a standardized uptake value. The PET images were transferred to our GK center in digital format.

GK-SRS Planning for the 2 Groups

The patients in the MRI group were judged to have recurrent lesions when the maximum diameter of the gadolinium-enhanced

Received for publication February 25, 2014; revision accepted July 2, 2014.

From the *Department of Neurosurgery, Tokyo Medical and Dental University, Tokyo, Japan; †Katsuta Hospital Mito Gamma House, Hitachi-naka, Japan; ‡Research Team for Neuroimaging, Tokyo Metropolitan Institute of Gerontology, Tokyo, Japan; and §Departments of Neurosurgery, Tokyo Women's Medical University Medical Center East, Tokyo, Japan.

Conflicts of interest and sources of funding: Supported by JSPS KAKENHI Grant No. 23390334.

Reprints: Tadashi Nariai, MD, PhD, Department of Neurosurgery, Graduate School, Tokyo Medical and Dental University, 1-5-45 Yushima, Bunkyo-ku, Tokyo 113-8519, Japan. E-mail: nariai.nsrg@tmd.ac.jp.

ISSN: 0363-9762/14/3911–0939